Antiferromagnetic order in systems with doublet $S_{tot}=1/2$ ground states

Sambuddha Sanyal, Argha Banerjee, Kedar Damle, and Anders W. Sandvik

Antiferromagnetic order in systems with doublet $S_{\text{tot}} = 1/2$ ground states

Sambuddha Sanyal,[1] Argha Banerjee,[1] Kedar Damle,[1] and Anders W. Sandvik[2]

[1]*Department of Theoretical Physics, Tata Institute of Fundamental Research, Mumbai 400005, India.*
[2]*Department of Physics, Boston University, 590 Commonwealth Avenue, Boston, Massachussetts 02215, USA.*

We use projector Quantum Monte Carlo methods to study the doublet ground states of two-dimensional $S = 1/2$ antiferromagnets on $L \times L$ square lattices with L odd. We compute the ground state spin texture $\Phi^z(\vec{r}) = \langle S^z(\vec{r}) \rangle_\uparrow$ in the ground state $|G\rangle_\uparrow$ with $S_{\text{tot}}^z = 1/2$, and relate n^z, the thermodynamic limit of the staggered component of $\Phi^z(\vec{r})$, to m, the thermodynamic limit of the magnitude of the staggered magnetization vector in the singlet ground state of the same system with L even. If the *direction* of the staggered magnetization in $|G\rangle_\uparrow$ were fully pinned along the $\hat{z}$ axis in the thermodynamic limit, then we would expect $n^z/m = 1$. By studying several different deformations of the square lattice Heisenberg antiferromagnet, we find instead that n^z/m is a universal function of m, independent of the microscopic details of the Hamiltonian, and well approximated by $n^z/m \approx 0.266 + 0.288m - 0.306m^2$ for $S = 1/2$ antiferromagnets. We define n^z and m analogously for spin-S antiferromagnets, and explore this universal relationship using spin-wave theory, a simple mean-field theory written in terms of the total spin of each sublattice, and a rotor model for the dynamics of the staggered magnetization vector. We find that spin-wave theory predicts $n^z/m \approx (0.987 - 1.003/S) + 0.0013m/S$ to leading order in $1/S$, while the sublattice-spin mean-field theory and the rotor model both give $n^z/m = S/(S+1)$ for spin-S antiferromagnets. We argue that this latter relationship becomes asymptotically exact in the limit of infinitely long-range *unfrustrated* exchange interactions.

I. INTRODUCTION AND OVERVIEW

Computational studies of strongly correlated systems necessarily involve an extrapolation to the thermodynamic limit from a sequence of finite sizes at which calculations are feasible. A detailed understanding[1] of these finite-size corrections is essential for obtaining accurate estimates of various quantities in the thermodynamic limit. For instance, the best estimates of m, the magnitude of the ground state Néel order parameter in the thermodynamic limit of the two-dimensional $S = 1/2$ square lattice Heisenberg antiferromagnet, are obtained by extrapolating to the thermodynamic limit from a sequence of periodic $L_x \times L_y$ systems with even length L_x (L_y) in the x (y) direction.[2,3] Other studies suggest[4] that it is sometimes advantageous to use "cylindrical" samples with periodic boundary conditions in one direction and pinned boundary conditions in the other direction, whereby spins are held fixed by the use of pinning fields on one pair of edges—this choice also allows for a very accurate determination of ground-state parameters such as m for specific values[4] of the aspect ratio L_y/L_x.

All these approaches focus on systems with an *even* number of spin-half variables; this choice allows the ground-state of the finite system to lie in the singlet sector favoured by unfrustrated antiferromagnetic interactions.[5] Although not commonly used, another choice is certainly possible: Namely, one could in principle consider antiferromagnets on a $L \times L$ square lattice with an odd number $N_{\text{tot}} = L^2$ of spin-half moments. By the Lieb-Mattis theorem[5], such a system is expected to have a doublet ground state with total spin $S_{\text{tot}} = 1/2$. Focusing on the $S_{\text{tot}}^z = 1/2$ member $|G\rangle_\uparrow$ of this doublet,

one could examine the ground state spin texture defined by $\Phi^z(\vec{r}) \equiv \langle S_{\vec{r}}^z \rangle_\uparrow$ (where $\langle \dots \rangle_\uparrow$ refers to expectation values in $|G\rangle_\uparrow$), and use the antiferromagnetic component of this spin texture, defined as

$$n^z = \lim_{N_{\text{tot}} \to \infty} \frac{1}{N_{\text{tot}}} \sum_{\vec{r}} \eta_{\vec{r}} \langle S_{\vec{r}}^z \rangle_\uparrow, \qquad (1)$$

to obtain information about the antiferromagnetic ordering in the system (here $\eta_{\vec{r}} = +1$ on the A sublattice and -1 on the B sublattice).

Clearly, n^z provides a measure of antiferromagnetic order that is quite distinct from the conventional order parameter m, which can be defined via

$$m^2 = \lim_{N_{\text{tot}} \to \infty} \frac{1}{N_{\text{tot}}} \sum_{\vec{r}\vec{r}'} \eta_{\vec{r}} \eta_{\vec{r}'} \langle \vec{S}_{\vec{r}} \cdot \vec{S}_{\vec{r}'} \rangle_0, \qquad (2)$$

where $\langle \dots \rangle_0$ denotes averages in the singlet ground states that obtain for N_{tot} even. The relationship between n^z and m is a fundamental aspect of the spontaneously broken $SU(2)$ symmetry of the Néel state. However, not much is known about it beyond the fact that n^z is *significantly smaller than* m for the nearest neighbour Heisenberg antiferromagnet on ths square lattice.[6]

Here, we provide a more detailed characterization of this relationship by studing three deformations of the nearest neighbour $S = 1/2$ square lattice Heisenberg antiferromagnet using projector Quantum Monte Carlo (QMC) methods. Our basic result is that the QMC data for n^z/m for these three models, when plotted against m, falls on a *single* curve which defines a universal function that is insensitive to the microscopic details of the

model Hamiltonian. We find that this universal function is well-approximated by a polynomial interpolation formula

$$n^z/m \approx 0.266 + 0.288m - 0.306m^2 \,. \qquad (3)$$

We also find that $\tilde{\Phi}^z(\vec{q})$, the Fourier transform of the full spin texture $\Phi^z(\vec{r})$, is peaked around the antiferromagnetic wave-vector $\mathbf{Q} = (\pi, \pi)$, with the shape of the peak at $\mathbf{Q}$ again being independent of microscopic details of the Hamiltonian.

Since the spin-length S at each site determines (via the Lieb-Mattis theorem) the representation of $SU(2)$ carried by the ground state multiplet of any suitably deformed spin-S Heisenberg antiferromagnet on the square lattice, these universal relationships are expected to depend sensitively on the value of S.

More precisely, although the ground state for L even is always a singlet for any S, the ground state for L odd is in the total spin S sector for any (unfrustrated or weakly frustrated) deformation of the spin-S Heisenberg antiferromagnet that continues to respect the Lieb-Mattis theorem. In this more general case, we may define $\Phi^z(\vec{r})$ as the expectation value of $S^z(\vec{r})$ in the $S_{\text{tot}} = S$, $S^z_{\text{tot}} = S$ ground state of an $L \times L$ system with L odd, and n^z as the thermodynamic limit of the antiferromagnetic part of $\Phi^z(\vec{r})$.

In this more general setting, our basic prediction is that n^z/m is a universal function of m that is insensitive to the microscopic details of the model Hamiltonian, but depends sensitively on S. In addition, we expect $\tilde{\Phi}^z(\vec{q})$ to have a universal peak around the antiferromagnetic vector $\mathbf{Q} = (\pi, \pi)$, with the shape of the peak depending sensitively on S.

By studying two quite different deformations of the spin-S square lattice Heisenberg antiferromagnet using spin-wave theory, we show that this universality of the peak at $\mathbf{Q}$ is captured by spin-wave theory to leading order in $1/S$. In addition, spin-wave theory yields the following prediction for the universal function n^z/m:

$$n^z/m = (1 - \alpha - \beta/S) + (\alpha/S)m + \mathcal{O}(S^{-2}), \quad (4)$$

with $\alpha \approx 0.013$ and $\beta \approx 1.003$. Thus, although leading order spin-wave theory captures qualitative features of the physics correctly, it is not a quantitatively good approximation to the $S = 1/2$ case.

Therefore, we explore two other ways of thinking about the universal function defined by n^z/m for general S. One of them is a mean field theory formulated in terms of the total spin of each sublattice, while the other approach is in terms of a quantum rotor Hamiltonian for $\hat{n}$, the *direction* of the Néel vector of a system with an odd number of sites. Both these give

$$n^z/m = \frac{S}{S+1} \qquad (5)$$

for spin-S antiferromagnets, which, in the $S = 1/2$ case, is close to the observed relationship, but not exactly
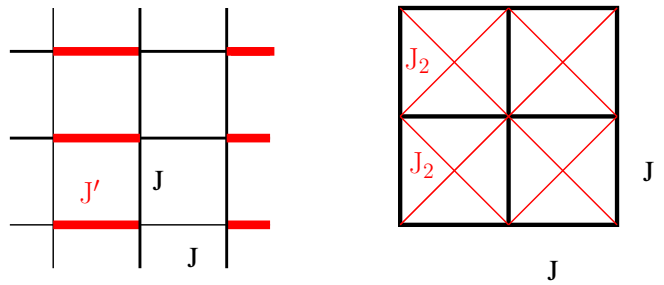

FIG. 1. An illustration of the interactions present in the JJ' (left panel) and JJ_2 (right panel) model Hamiltonians. In this illustration, black bonds denote exchange interaction strength of J, while a red bond represents exchange strength of J' (J_2) in the left (right) panel

right. We argue that this latter estimate (Eqn. 5) will become asymptotically exact for a spin-S antiferromagnet in the limit of infinitely long-range *unfrustrated* exchange interactions. In this limit, we also expect $m \to S$, since the antiferromagnetic order is expected to be perfect in this limit. With this in mind, our polynomial fit to the $S = 1/2$ QMC data (Eqn. 3) for n^z/m was constrained to ensure that $n^z/m \to 1/3$ when $m \to 1/2$—in other words, our polynomial fit used only *two* independent coefficients.

The outline of the rest of the paper is as follows: In Section II we define various deformations of the square lattice $S = 1/2$ Heisenberg antiferromagnet. In Section III, we outline the projector quantum Monte Carlo (QMC) method used in this study, and then discuss in some detail our QMC results for n^z as well as the full spin texture $\Phi^z(\vec{r})$, focusing on the universal properties alluded to earlier. In Section IV, we outline three analytical (but approximate) approaches to the relationship between n^z and m. The first is a large-S spin-wave expansion. The second is a mean-field theory formulated in terms of the total spin of each sublattice. And the third approach is in terms of a quantum rotor Hamiltonian which is expected to correctly describe the low-energy tower of states for odd N_{tot}. In Section V, we conclude with some speculations about a possible effective field theory approach to the calculation of $\Phi^z(\vec{r})$. Some technical details are relegated to the appendix so as to not interrupt the flow of our presentation.

II. MODELS

We consider four deformations of the square lattice $S = 1/2$ nearest neighbour Heisenberg antiferromagnet; all four retain the full $SU(2)$ spin rotation symmetry of the original model.

The first of these models is the coupled-dimer antiferromagnet, in which there are two kinds of nearest neighbour interactions J and J', as shown in Fig. 1 (left panel), where the ratio $\alpha = J'/J$ can be tuned from $\alpha = 1$ to
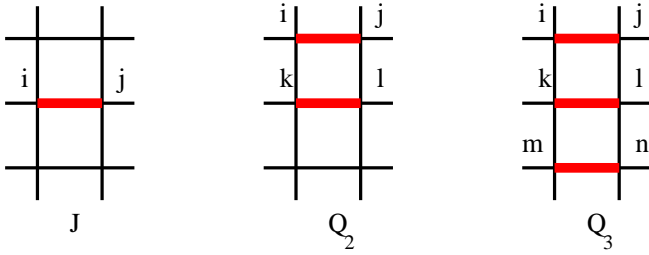
FIG. 2. Bond and plaquette operators in JQ model Hamiltonians. A thick bond denotes a bipartite projector acting on that bond. All possible orientations of these bond and plaquette operators are allowed.

$\alpha = \alpha_c \approx 1.90$ at which collinear antiferromagnetic order is lost.[7] The Hamiltonian for this system reads:

$$H_{JJ'} = J\sum_{\langle ij\rangle} \mathbf{S}_i \cdot \mathbf{S}_j + J'\sum_{\langle ij\rangle'} \mathbf{S}_i \cdot \mathbf{S}_j, \qquad (6)$$

where $\langle ij\rangle$ ($\langle ij\rangle'$) denotes a pair of nearest neighbour sites connected by a black (red) bond (see Fig. 1). Another deformation of the Heisenberg model, the JJ_2 model, has additional next nearest neighbour Heisenberg exchange interactions J_2, as shown in Fig. 1 (right panel). The Hamiltonian reads

$$H_{JJ_2} = J\sum_{\langle ij\rangle} \mathbf{S}_i \cdot \mathbf{S}_j + J_2\sum_{\langle\langle ij\rangle\rangle} \mathbf{S}_i \cdot \mathbf{S}_j, \qquad (7)$$

where $\langle\langle ij\rangle\rangle$ denotes a pair of next nearest neighbour sites. Both these are amenable to straightforward spin-wave theory analyses, and the coupled dimer model can also be studied numerically at large sizes using unbiased and extremely accurate QMC methods due to the absence of any sign problems. However, exact numerical results on the JJ_2 model are restricted to small sizes since QMC methods encounter a sign problem when dealing with next-nearest neighbour interactions on the square lattice.

In addition, we study two generalizations that involve additional multispin interactions; the "JQ" models.[8,9] Of these, the JQ_2 model has 4-spin interactions in addition to the usual Heisenberg exchange terms, and is defined by the Hamiltonian

$$H_{JQ_2} = -J\sum_{\langle ij\rangle} P_{ij} - Q_2 \sum_{\langle ij,kl\rangle} P_{ij}P_{kl}, \qquad (8)$$

where the plaquette interaction Q_2 involves two adjacent parallel bonds on the square lattice as shown in Fig. 2 (middle panel) and

$$P_{ij} = \frac{1}{4} - \mathbf{S}_i \cdot \mathbf{S}_j \qquad (9)$$

is a bipartite singlet projector. Note that the first term in Eqn. 8 is just the standard antiferromagnetic Heisenberg exchange term (apart from a constant). Similarly, the
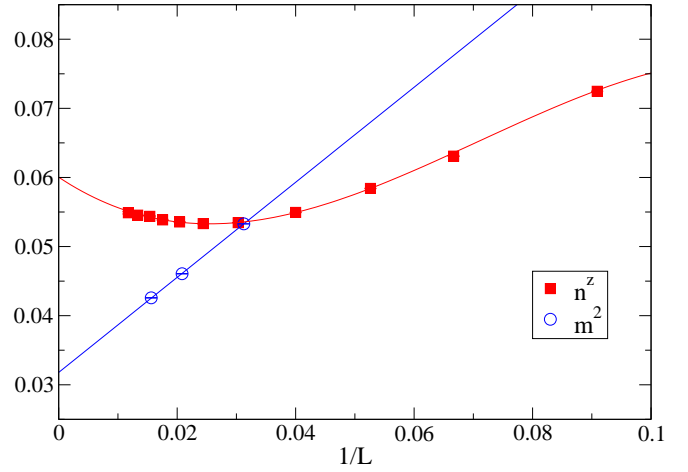

FIG. 3. An illustrative example of finite size corrections of n^z and m^2, observed in the antiferromagnetic phase of the JJ' model($J' = 1.8$). Note the non-monotonic behaviour of finite size corrections for n^z, which is fitted to a cubic polynomial.
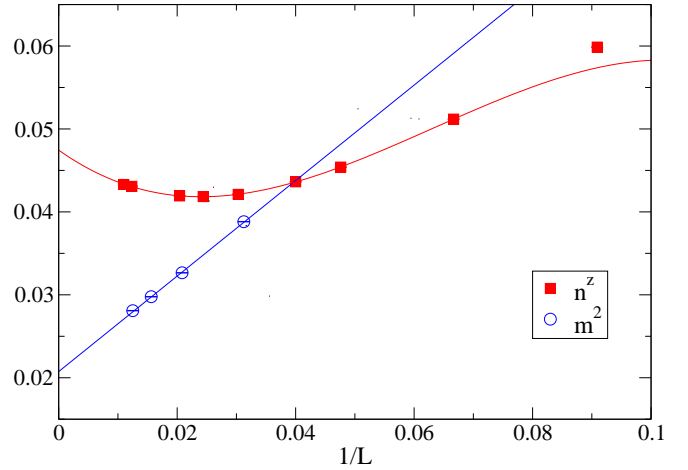

FIG. 4. Another illustrative example of finite size corrections of n^z and m^2, observed in the antiferromagnetic phase of JQ_2 model at $Q_2 = 1.0$. Again, note the non-monotonic behaviour of finite size corrections for n^z, which is fitted to a cubic polynomial (only $L > 20$ data used in the fit). In contrast, finite size data for m^2 is well described by a linear dependence on $1/L$.

JQ_3 model has 6-spin interactions and is defined by the Hamiltonian

$$H_{JQ_3} = -J\sum_{\langle ij\rangle} P_{ij} - Q_3 \sum_{\langle ij,kl,nm\rangle} P_{ij}P_{kl}P_{nm}, \quad (10)$$

where the plaquette interactions now involve three adjacent parallel bonds on the square lattice, as shown in Fig. 2 (right panel). The products of singlet projectors making up the Q_2 and Q_3 terms tend to reduce the Néel order of the ground state, and, when sufficiently strong, lead to a quantum phase transition into a valence-bond-
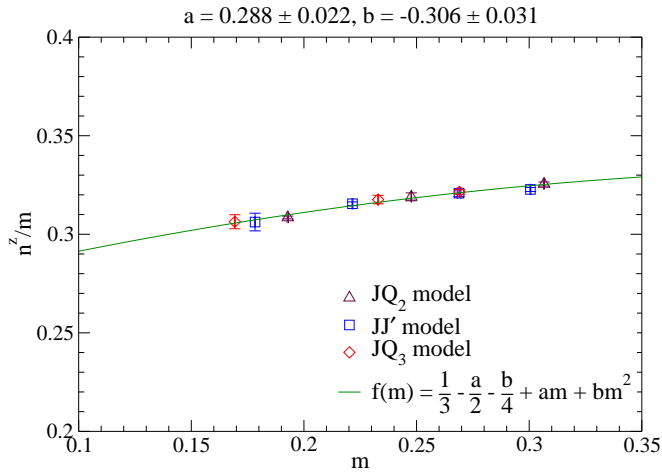
FIG. 5. Extrapolated thermodynamic values of n^z for three different models of antiferromagnets on an open lattice, plotted as function of staggered magnetisation m for the same models on periodic lattices. The former is clearly an universal function of the later. This universal function can be well approximated by a polynomial fit constrained to ensure that $n^z(m) \to m/3$ in the limit of $m \to \frac{1}{2}$: $n^z \approx (1/3 - a/2 - b/4)m + am^2 + bm^3$, with $a \approx 0.288$ and $b \approx -0.306$.

solid state.[8,9] Here we stay within the Néel state in both models, and study universal aspects of this state as the Néel order is weakened.

III. PROJECTOR QMC STUDIES

We use the $S_{\text{tot}} = 1/2$ sector generalization[10] of the valence-bond basis projector QMC method[11,12] to study $L \times L$ samples with L odd and free boundary conditions. We compute $\Phi^z(\vec{r})$ and n^z in such samples for the JJ' model and JQ models in their antiferromagnetic phase. We also study the same models on $L \times L$ lattices with L even and periodic bondary conditions using the original singlet sector valence bond projector QMC method.[11,12] In both cases we use the most recent formulation with very efficient loop updates.[10,12] Our system sizes range from $L = 11$ to $L = 101$, and projection power scales as L^3 to ensure convergence to the ground state. We perform $\gtrsim 10^5$ equilibration steps followed by $\gtrsim 10^6$ Monte Carlo measurements to ensure that statistical and systematic errors are small.

Data for n^z from a sequence of $L \times L$ systems with L odd shows that n^z extrapolates to a finite value in the $L \to \infty$ limit as long as the system is in the antiferromagnetic phase. However, we find that the approach of this observable to the thermodynamic limit has a non-monotonic behaviour. To obtain accurate extrapolations to infinite size, it is therefore necessary to fit the finite size data to a third-order polynomial in $1/L$. We find that the coefficient for the leading $1/L$ term in this polynomial is rather small; this is true for all the models studied here,

as long as they remain in the antiferromagnetic phase. In Fig.. 3 and Fig. 4, we show examples of this behaviour of the finite size corrections in n^z. In these figures, we also show the approach to the thermodynamic limit for m, as measured in a sequence of periodic $L \times L$ systems with L even. In contrast to the behaviour of n^z, m extrapoloates monotonically to the thermodynamic limit, with a dominant $1/L$ dependence—this is consistent with previous studies of the structure factor in square lattice antiferromagnets[12] (however, with spatially anisotropic couplings, one can also observe strong non-monotonicity in m[13]).

The non-zero value of n^z in the large L limit clearly reflects the long-range antiferromagnetic order present in the system. For periodic systems with even L, the same long range antiferromagnetic order is captured by the non-zero value of m in the large L limit. One can view m as the magnitude of the Néel vector in the thermodynamic limit. From this perspective, n^z/m is a measure of the extent to which the Néel vector is "pinned" in the thermodynamic limit to lie along the $+\hat{z}$ axis in the $S_{\text{tot}}^z = 1/2$ ground state of a system with odd L. Thus, the ratio n^z/m is a fundamental aspect of the spontaneous symmetry breaking in the antiferromagnetic state. It is therefore interesting to ask: What is the relationship between these two measures of antiferromagnetic order? Our numerical data are unequivocal as far as this relationship is concerned, as is clear from Fig. 5, which shows a plot of n^z/m versus m in the thermodynamic limit of the JJ', JQ_2 and JQ_3 models. Here *each* point represents the result of a careful extrapolation similar to the examples shown in Fig. 3 and Fig. 4, and provides an accurate estimate of the corresponding thermodynamic limits for n^z and m. From this figure, it is clear that n^z/m is a universal function of m independent of the microscopic structure of the Hamiltonian. To model this universal function, we use a polynomial fit that is constrained to ensure that $n^z \to \frac{m}{3}$ when $m \to \frac{1}{2}$; the rationale for this constraint will become clear in Sec. IV. We find (Fig. 5) that the QMC results for the dependence of n^z/m on m are fit well by the following functional form:

$$n^z/m = \left(\frac{1}{3} - \frac{a}{2} - \frac{b}{4}\right) + am + bm^2 \,, \qquad (11)$$

with $a \approx 0.288$ and $b \approx -0.306$.

If one views this universal relationship as being a property of the low energy effective field theory of the antiferromagnetic phase, one is led to expect that the full spatial structure of the spin texture $\Phi^z(\vec{r})$ should also be universal in some sense. More precisely, one is led to expect that $\tilde{\Phi}^z(\vec{q})$, the Fourier transform of $\Phi^z(\vec{r})$, should be peaked at the antiferromagnetic vector $\mathbf{Q} = (\pi, \pi)$, with a universal shape in the vicinity of this peak.

To test this, we compare our data for $\tilde{\Phi}^z(\vec{q})$ in the JJ' model and the JQ_3 model, choosing the strengths of the J' interaction and the Q_3 interaction so that both have the same value of m, and therefore the same value of n^z. This is shown in Fig. 6, which shows that
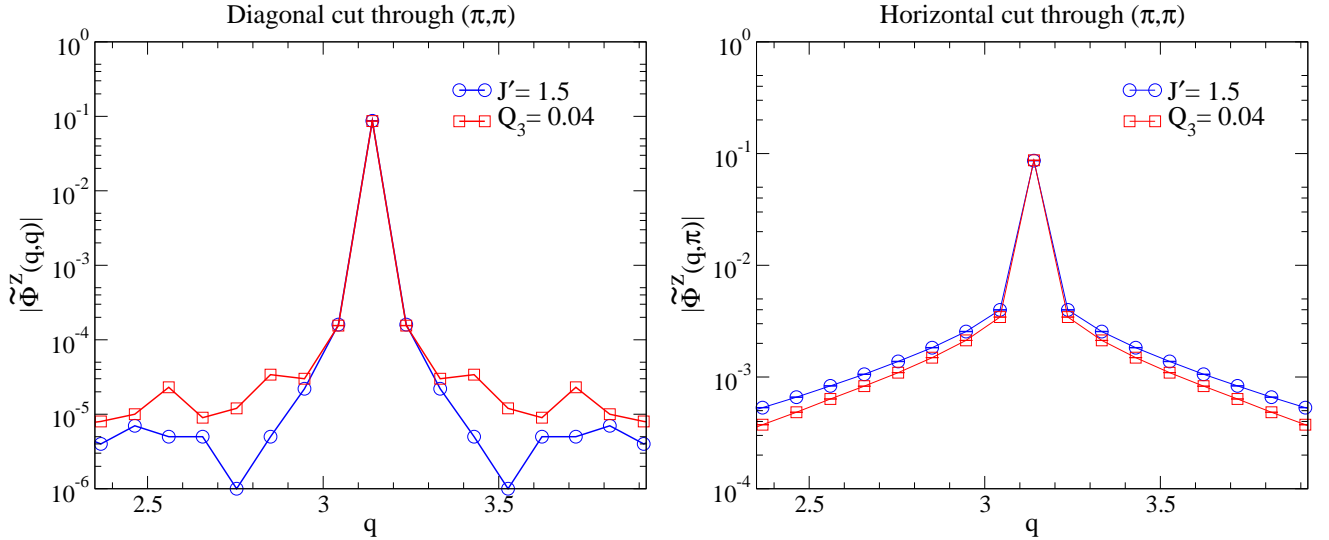
FIG. 6. QMC Results: Fourier transform (with antiperiodic boundary conditions assumed for convenience) of the QMC results for $\Phi^z(\vec{r})$ (for JJ' and JQ_3 model with $L = 65$, $S = 1/2$) along cuts passing through the antiferromagnetic wavevector $\mathbf{Q} = (\pi, \pi)$. Note the universality of the results in the neighbourhood of the antiferromagnetic wavevector, which in any case accounts for most of the weight in Fourier space.

these very different microscopic Hamiltonians have spin-textures whose Fourier transform falls on top of each other at and around the antiferromagnetic wavevector.

IV. ANALYTICAL APPROXIMATIONS

We now present three analytical approaches aimed at understanding these numerical results presented in the previous section: First, we develop a spin-wave expansion that becomes asymptotically exact for large S[14]. Second, we explore a mean-field theory written in terms of the total spin of each sublattice. Finally, we describe an alternative approach in which the low-energy antiferromagnetic tower of states of a spin-1/2 antiferromagnet is described by a phenomenological rotor model[17] adapted to the case of a system with odd $N_{\rm tot}$.

A. Spin-wave expansion

The leading order spin-wave calculation proceeds as usual by using an approximate representation of spin operators in terms of Holstein-Primakoff bosons. The resulting bosonic Hamiltonian is truncated to leading (quadratic) order in boson operators to obtain the first quantum corrections to the classical energy of the system.

As is standard in the spin-wave theory of Néel ordered states, we start with the classical Néel ordered configuration with the Néel vector pointing along the $\hat{z}$ axis, which corresponds to $S^z_{\vec{r}} = \eta_{\vec{r}}S$. We then represent the spin operators at a site $\vec{r}$ of the square lattice in terms of canonical bosons to leading order in S as follows: For

sites $\vec{r}$ belonging to the A sublattice we write

$$S^+_{\vec{r}} = \sqrt{2S}b_{\vec{r}} ; \quad S^z_{\vec{r}} = S - b^\dagger_{\vec{r}}b_{\vec{r}} , \qquad (12)$$

while on sites $\vec{r}$ belonging to the B sublattice we write

$$S^-_{\vec{r}} = \sqrt{2S}b_{\vec{r}} ; \quad S^z_{\vec{r}} = -S + b^\dagger_{\vec{r}}b_{\vec{r}} . \qquad (13)$$

The number of bosons at each site thus represents the effect of quantum fluctuations away from the classical Néel ordered configuration.

To quadratic order in the boson operators, this expansion yields the following spin-wave Hamiltonian in the general case (with arbitrary two-spin exchange couplings):

$$H_{sw} = \epsilon_{cl}S^2 + \frac{S}{2}\mathbf{b}^\dagger M\mathbf{b} , \text{ with}$$

$$M_{\vec{r}\vec{r}'} = \begin{pmatrix} A_{\vec{r}\vec{r}'} & B_{\vec{r}\vec{r}'} \\ B_{\vec{r}\vec{r}'} & A_{\vec{r}\vec{r}'} \end{pmatrix}$$

$$\mathbf{b}_{\vec{r}} = \begin{pmatrix} b_{\vec{r}} \\ b^\dagger_{\vec{r}} \end{pmatrix} . \qquad (14)$$

Here $\epsilon_{cl}S^2$ is the classical energy of the Néel state, M in the first line is a $2N_{\rm tot}$ dimensional matrix specified in terms of $N_{\rm tot}$ dimensional blocks A and B, and $\mathbf{b}$ is a $2N_{\rm tot}$ dimensional column vector as indicated above. Elements of A and B can be written explicitly as

$$A_{\vec{r}\vec{r}'} = (Z^U_{\vec{r}} - Z^F_{\vec{r}})\delta_{\vec{r}\vec{r}'} + J^F_{\vec{r}\vec{r}'}, \qquad (15)$$

$$B_{\vec{r}\vec{r}'} = J^U_{\vec{r}\vec{r}'}. \qquad (16)$$

In the above, $J^F_{\vec{r}\vec{r}'}$ are Heisenberg exchange couplings between two sites $\vec{r}$ and $\vec{r}'$ belonging to the same sublattice, $J^U_{\vec{r}\vec{r}'}$ are the Heisenberg exchange couplings between sites
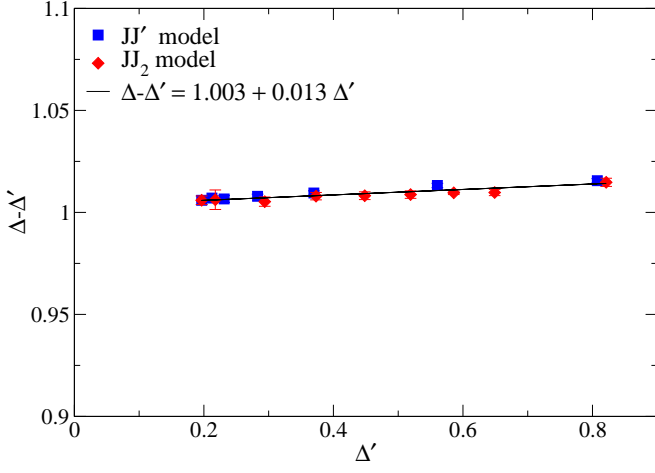
FIG. 7. $\Delta - \Delta'$, the difference between the leading spin-wave corrections to n^z and m, plotted against the leading spin-wave corrections Δ' to m for the JJ' and JJ_2 models described in the text.

belonging to different sublattices, and

$$Z_{\vec{r}}^U = \sum_{\vec{r}'} J_{\vec{r}\vec{r}'}^U, \qquad (17)$$

$$Z_{\vec{r}}^F = \sum_{\vec{r}'} J_{\vec{r}\vec{r}'}^F. \qquad (18)$$

The effects of quantum fluctuations on the classical Néel state can now be calculated by diagonalizing this Hamiltonian by a canonical Bogoliubov transformation. For periodic $L \times L$ samples with L even, it is possible to exploit the translational invariance of the problem and work in Fourier space to obtain these spin-wave modes and their wavefunctions and use this information to calculate m by noting that

$$m = S - \lim_{N_{\text{tot}} \to \infty} \frac{1}{N_{\text{tot}}} \sum_{\vec{r}} \langle b_{\vec{r}}^\dagger b_{\vec{r}} \rangle_{pbc} \qquad (19)$$

where the expectation value is taken in the ground state of the quadratic Hamiltonian H_{sw} with periodic boundary conditions, and the limit is taken from a sequence of sizes with even N_{tot}. In the thermodynamic limit, this gives the leading order spin-wave results for m

$$m = S - \Delta' \qquad (20)$$

As these results are standard and well-known,[15] we do not provide further details here.

To obtain the spin-wave expansion result for n^z, we need to repeat the same calculation for $L \times L$ samples with free boundary conditions and L odd (i.e., and take the thermodynamic limit:

$$n^z = S - \lim_{N_{\text{tot}} \to \infty} \frac{1}{N_{\text{tot}}} \sum_{\vec{r}} \langle b_{\vec{r}}^\dagger b_{\vec{r}} \rangle_{obc} \qquad (21)$$

where the expectation value is taken in the ground state of the quadratic Hamiltonian H_{sw} with open boundary

conditions, and the limit is taken from a sequence of samples with odd N_{tot} (i.e. with N_A, the number of A sublattice sites, exceeding N_B, the number of B sublattice sites by one: $N_A = N_B + 1$). Results for the spin-wave modes for such samples do not seem to be available in the literature. We therefore discuss the corresponding analysis in detail in the Appendix A.

In the thermodynamic limit, this analysis finally yields the result

$$n^z = S - \Delta \qquad (22)$$

where Δ represents the leading spin-wave correction to the classical value for n^z. In order to obtain n^z reliably in this manner, it is important to understand the finite size corrections to Δ for various values of J'/J in the striped interaction model and J_2/J in the model with next-nearest neighbour interactions, and use this understanding to reliably extrapolate to the thermodynamic limit. This analysis of finite-size corrections is detailed in the Appendix B.

Using such finite-size extrapolations to the thermodynamic limit, we obtain Δ for various values of J_2/J and J'/J, and then compare the results with those for Δ' obtained directly in the thermodynamic limit by standard analytical techniques. Specifically, we ask if the universality seen in our QMC results is reflected in these leading order spin-wave corrections to n^z and m. The answer is provided by Fig. 7, which shows that the numerically obtained spin-wave corrections apparently satisfy a universal linear relationship

$$\Delta - \Delta' \approx 1.003 + 0.013\Delta' \qquad (23)$$

as one deforms away from the pure square lattice antiferromagnet in various ways.

What does this imply for the ratio n^z/m to leading order in $1/S$? To answer this, we note that

$$\frac{n^z}{m} = 1 - \frac{\Delta - \Delta'}{S} + \mathcal{O}(S^{-2}) \qquad (24)$$

Using our numerically established universal relationship between $\Delta - \Delta'$ and Δ' and the formula for m in terms of Δ', we obtain the universal relationship

$$n^z = \alpha m + \beta m^2 \qquad (25)$$

with $\alpha \approx 0.987 - 1.003/S$ and $\beta \approx 0.013/S$. Thus, spin-wave theory correctly predicts that n^z/m is a universal function of m that depends sensitively on the value of spin-length S at each site. However, being a large-S expansion, it is unable to give a quantitatively correct prediction for the form of this universal function at $S = 1/2$ case.

Finally, we use our spin-wave predictions for the ground-state spin texture to look at the Fourier transform of the spin-texture for various deformations of the pure antiferromagnet. The results are shown in Fig. 8, which demonstrates that spin-wave theory also predicts

that the Fourier transform of the spin-texture near the antiferromagnetic wave-vector is a universal function of the wavevector; this provides some rationalization for the observed universality of the Fourier transformed spin texture seen in our QMC numerics.

B. Sublattice-spin mean-field theory

We now turn to a simple mean-field picture in terms of the dynamics of the total spins $\vec{L}_A$ and $\vec{L}_B$ of the A and B sublattices respectively for an antiferromagnet composed of spin-S moments at each site. The idea of this mean-field theory is to approximate the true low-energy spectrum of the spin-S antiferromagnet by that of a model in which the N_A A-sublattice spins form a giant moment $\vec{L}_A$ that couples antiferromagnetically with a similar giant moment $\vec{L}_B$ formed by the N_B B-sublattice spins.

When $N_A = N_B + 1$, it is clearly appropriate to set the total spin quantum number of $\vec{L}_B$ to $S_B \equiv SN_B$ and the total spin quantum number of $\vec{L}_A$ to $S_A \equiv SN_A = S_B + S$. In this mean-field treatment, we assume that the dynamics of $\vec{L}_A$ and $\vec{L}_B$ is described a low-energy effective Hamiltonian

$$H_{MF} = J_{MF}\vec{L}_A \cdot \vec{L}_B \qquad (26)$$

with $J_{MF} > 0$. Within this mean-field treatment, the $S_{\text{tot}} = S$ ground state multiplet expected from the Lieb-Mattis theorem is thus modeled by the $S_{\text{tot}} = S$ multiplet obtained by the quantum mechanical addition of angular momenta $S_B \equiv SN_B$ and $S_A = S_B + S$. Within this mean-field theory, n^z is modeled in terms of the expectation value of $L_A^z - L_B^z$ in the $S_{\text{tot}}^z = S$ state of this multiplet:

$$n^z = \lim_{N_{\text{tot}}\to\infty} \frac{1}{N_{\text{tot}}}\langle S_{\text{tot}} = S\,,\, S_{\text{tot}}^z = S\,;\, S_B\,,\, S_A|(L_A^z - L_B^z)|S_{\text{tot}} = S\,,\, S_{\text{tot}}^z = S\,;\, S_B\,,\, S_A\rangle\,. \qquad (27)$$

Using the standard result for the minimum angular momentum state obtained by the quantum mechanical addition of two angular momenta, this can be written as:

$$n^z = \lim_{N_B\to\infty} \frac{2S+1}{2N_B+1} \sum_{m=-(S_B-S)}^{S_A} \frac{(2m-S)\Gamma(2S_B+1)\Gamma(S_A+m+1)}{\Gamma(2S_A+2)\Gamma(S_B+m+1-S)} \qquad (28)$$

Perhaps surprisingly, this sum can be carried out in closed form, to give the result

$$n^z = \lim_{N_B\to\infty} \frac{1}{2N_B+1}(S + \frac{2S}{S+1}S_B) \qquad (29)$$

On the other hand, we may also calculate m^2 defined within this approach as

$$m^2 = \lim_{N_{\text{tot}}\to\infty} \frac{1}{N_{\text{tot}}^2}\langle(\vec{L}_A - \vec{L}_B)^2\rangle_{\text{singlet}} \qquad (30)$$

where the average is taken in the $S_{\text{tot}} = 0$ singlet state obtained by the quantum mechanical addition of $\vec{L}_A$ and $\vec{L}_B$ where the two sublattice angular momenta are now equal: $S_B = S_A = SN_{\text{tot}}/2$ for a sample with an even number of sites N_{tot}. This gives

$$m = \lim_{N_{\text{tot}}\to\infty} \frac{1}{N_{\text{tot}}}2\sqrt{S_B(S_B+1)}\,. \qquad (31)$$

From these results for n^z and m, we obtain the following prediction for their ratio n^z/m in the thermodynamic limit:

$$n^z/m = \frac{S}{S+1} \qquad (32)$$

Is there a limit in which this sublattice-spin mean-field theory is expected to give exact results? To answer this, we note that the sublattice-spin mean-field theory gives the exact spectrum of an infinite-range model with spin-S moments at each site in which *every* A-sublattice spin interacts with *every* B-sublattice spin via a *constant* (independent of distance) antiferromagnetic exchange coupling J_{MF}.

Thus, our mean-field theory is expected to become asymptotically exact in the limit of infinitely long-range *unfrustrated* couplings. In this limit, we expect $m \to S$ and $n^z \to S^2/(S+1)$—in other words, we expect n^z/m to equal $S/S+1$ when m tends to S. This is the constraint (with S set equal to $1/2$) that we built into our choice of polynomial fit of our QMC data for n^z/m in Sec. III.

C. Quantum rotor Hamiltonian

When any continuous symmetry is broken, the corresponding order parameter variable becomes very "heavy" in a well-defined sense.[14] The long-time, slow dynamics of this heavy nearly classical variable is controlled by an effective "mass" that diverges in the thermodynamic limit.

For a Néel ordered magnet, the slow degree of freedom is $\hat{n}$, the direction of the Néel vector in spin space. In the
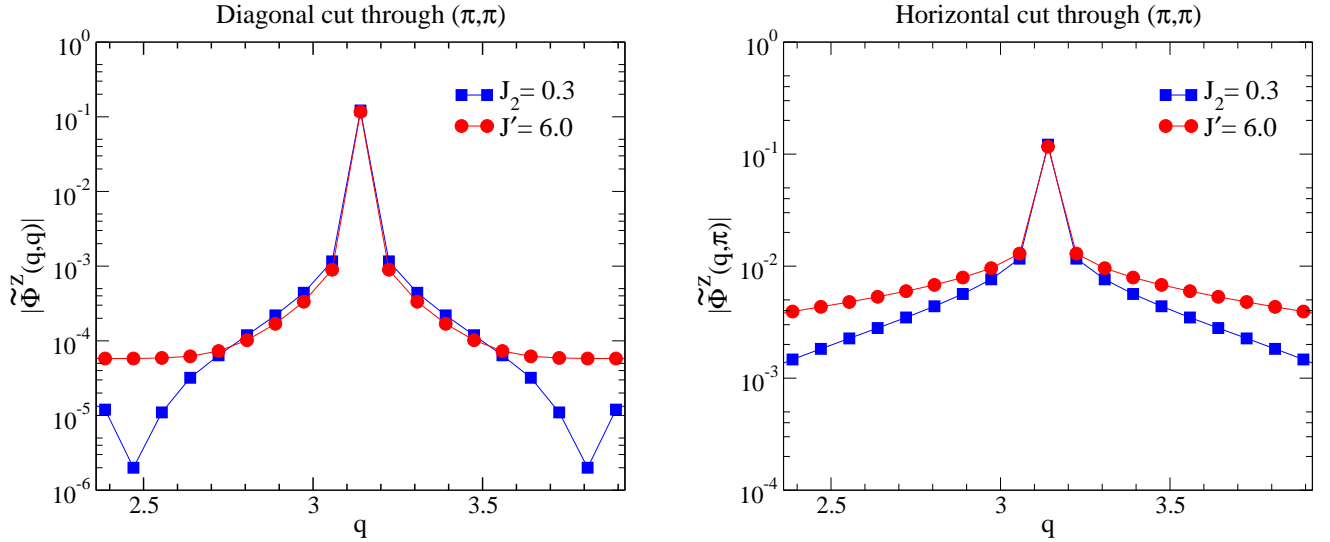
FIG. 8. Fourier transform (with antiperiodic boundary conditions assumed for convenience) of the spin-wave result for $\Phi^z(\vec{r})$ (assuming $S = 3/2$ and calculated using $L = 75$ for JJ_2 and JJ' model) along cuts passing through the antiferromagnetic wavevector (π, π). Note the nearly universal nature of the results in the neighbourhood of the antiferromagnetic wavevector, which in any case accounts for most of the weight of the transformed signal.

usual case of an antiferromagnet with an even number of $S = 1/2$ moments, the low-energy effective Hamiltonian that controls this slow orientational dynamics of the Néel vector is

$$H_{\text{rotor}} = \frac{\vec{L} \cdot \vec{L}}{2\chi N_{\text{tot}}} \qquad (33)$$

where $\vec{L}$ is the angular momentum conjugate to the "quantum rotor" coordinate $\hat{n}$, χ is the uniform susceptibility per spin, and N_{tot} is the total number of sites.

Here, we generalize this to the case with $N_A = N_B + 1$ and $N_{\text{tot}} = 2N_B + 1$. To identify the appropriate generalization, we follow earlier work on quantum rotor descriptions of insulating antiferromagnets doped with a single mobile charge-carrier.[17] By analogy to this case, we postulate that the correct rotor description of our problem is in terms of a rotor Hamiltonian in which $\vec{L}$ is replaced by the angular momentum operator $\vec{L}'$ conjugate to a quantum rotor coordinate $\hat{n}$ that now parametrizes a unit-sphere with a magnetic monopole of dimensionless strength S at its origin.[18] In other words, we postulate a low-energy effective Hamiltonian

$$H_{\text{rotor}}^{(S)} = \frac{\vec{L}' \cdot \vec{L}'}{2\chi N_{\text{tot}}} \qquad (34)$$

where the superscript reminds us that the lowest allowed angular momentum quantum number l of the modified angular momentum operator $\vec{L}'$ is $l = S$.

In the notation of Ref 18, the angular wavefunction of the $l = S$, $m_l = S$ ground state of this modified rotor Hamiltonian is the *monopole harmonic* $Y_{-S,S,S}(\theta, \phi)$. To model n^z/m, we must compute the expectation value of

$\hat{n}^z \equiv \cos(\theta)$ in this monopole harmonic wavefunction on the unit sphere. Since

$$|Y_{-S,S,\pm S}(\theta, \phi)|^2 \propto (1 \pm \cos(\theta))^{2S} , \qquad (35)$$

we obtain

$$n^z/m = \frac{S}{S + 1} . \qquad (36)$$

Thus, this apparently more general phenomenology, which ignores non-zero wavevector modes as well as amplitude fluctuations of the Néel order parameter, but makes no assumptions about long-range interactions, reproduces the results of the sublattice-spin mean-field theory that is exact in the limit of infinite-range unfrustrated interactions. This is perhaps not entirely surprising given that Anderson's original analysis[14] of the low energy tower of states in an antiferromagnet used a picture in terms of the total spin of each sublattice to arrive at a rotor description.

In any case, since our QMC data for $S = 1/2$ show clear deviations from the prediction $n^z/m = S/(S+1)$ in the $S = 1/2$ case, we conclude that non-zero wavevector modes of the Néel order parameter are essential for a correct calculation of the universal function n^z/m within a quantum rotor model of the antiferromagnetic phase.

V.   DISCUSSION

A natural question that arises from our results is whether the universal ground state spin texture we have found here can be successfully described using an effective

field theory approach of the type used recently by Eggert and collaborators for studying universal aspects of the alternating order induced by missing spins in two dimensional $S = 1/2$ antiferromagnets.[19] This approach uses a non-linear sigma-model description of the local antiferromagnetic order parameter, with lattice scale physics only entering via the values of the stiffness constant ρ_s and the transverse susceptibility $\chi_\perp$, and the presence of the vacancy captured by a local term in the action. An analogous treatment for our situation would need two things—one is a way of restricting attention to averages in the $S_{\text{tot}} = 1/2$ component $|G\rangle_\uparrow$ of the ground state doublet, and the other is an understanding of the right boundary conditions or boundary terms in the action, so as to correctly reflect that fact that our finite sample has open boundaries. We leave this as an interesting direction for future work, which may shed some light on the role of non-zero wavevector modes that were left out of the rotor description of the earlier section. Finally, we note that it might be quite interesting to analyze the leading order spin-wave theory results for n^z/m more deeply to understand exactly how the spin-wave theory result for n^z/m ends up being universal despite the fact that it most likely receives significant contributions from modes away from the extreme long-wavelength limit.

VI. ACKNOWLEDGEMENTS

Appendix A: Spin-wave theory with open boundary conditions and odd N_{tot}

The effects of quantum fluctuations on the classical Néel state can be calculated by diagonalizing the quadratic spin-wave Hamiltonian by a canonical Bogoliubov transformation $\mathbb{S}$ which relates the Holstein-Primakoff bosons b to the bosonic operators γ corresponding to spin-wave eigenstates

$$\mathbf{b} = \mathbb{S}\Gamma, \qquad \Gamma_\mu = \begin{pmatrix} \gamma_\mu \\ \gamma_\mu^\dagger \end{pmatrix} , \qquad (A1)$$

where $\mathbb{S}$ is a $2N_{\text{tot}}$ dimensional matrix that transforms from $\mathbf{b}$ which creates and destroys bosons at specific lattice sites $\vec{r}$ to Γ which creates and destroys spin-wave quanta in specific spin-wave modes μ. Naturally, we must

require that H_{sw} be *diagonal* in this new basis. We represent this diagonal form as

$$H_{sw} = \epsilon_{cl}S^2 + \frac{S}{2}\Gamma^\dagger D\Gamma , \qquad (A2)$$

where

$$D = \begin{pmatrix} \Lambda & 0 \\ 0 & \Lambda \end{pmatrix}, \qquad (A3)$$

with Λ denoting the diagonal matrix with the N_{tot} positive spin-wave frequencies λ_μ on its diagonal.

To construct a $\mathbb{S}$ that diagonalizes H_{sw} in the Γ basis, we look for $2N_{\text{tot}}$ dimensional column vectors

$$y^\mu = \begin{pmatrix} u^\mu \\ v^\mu \end{pmatrix}, \qquad (A4)$$

which satisfy the equation

$$My^\mu = \epsilon_\mu \mathcal{I}y^\mu \qquad (A5)$$

with *positive* values of ϵ_μ equal to the positive spin-wave frequencies λ_μ for $\mu = 1, 2, 3 \ldots N_{\text{tot}}$. Here u^μ and v^μ are N_{tot} dimensional vectors,

$$\mathcal{I} = \begin{pmatrix} \mathbf{1} & \mathbf{0} \\ \mathbf{0} & -\mathbf{1} \end{pmatrix}, \qquad (A6)$$

and $\mathbf{1}$ is the $N_{\text{tot}} \times N_{\text{tot}}$ identity matrix. With these y^μ in hand, one may obtain N_{tot} additional solutions to Eqn. A5, this time with *negative* $\epsilon_{N_{\text{tot}}+\mu} = -\lambda_\mu$ by interchanging the roles of the N_{tot} dimensional vectors u_μ and v_μ in this construction. In other words, we have

$$y^{N_{\text{tot}}+\mu} = \begin{pmatrix} v^\mu \\ u^\mu \end{pmatrix}, \qquad (A7)$$

with $\mu = 1, 2, 3 \ldots N_{\text{tot}}$.

We now construct $\mathbb{S}$ by using these y^μ (with $\mu = 1, 2, 3 \ldots 2N_{\text{tot}}$) as its $2N_{\text{tot}}$ columns:

$$\mathbb{S} = \left(y^1, y^2, y^3 \ldots y^{2N_{\text{tot}}} \right) . \qquad (A8)$$

Clearly, this choice of $\mathbb{S}$ satisfies the equation

$$M\mathbb{S} = \mathcal{I}\mathbb{S}\mathcal{I}D \qquad (A9)$$

Furthermore, the requirement that the Bogoliubov transformed operators γ obey the same canonical bosonic commutation relations as the b operators implies that $\mathbb{S}$ must satisfy

$$\mathbb{S}^\dagger \mathcal{I}\mathbb{S} = \mathcal{I} , \qquad (A10)$$

This constraint is equivalent to "symplectic" orthonormalization conditions:

$$(u^\mu)^\dagger u^\nu - (v^\mu)^\dagger v^\nu = \delta_{\mu\nu} , \qquad (A11)$$
$$(u^\mu)^\dagger v^\nu - (v^\mu)^\dagger u^\nu = 0 ,$$

for $\mu, \nu = 1, 2, 3 \ldots N_{\text{tot}}$. It is now easy to see that Eqn A9 and Eqn A10 guarantee that H_{sw} is indeed diagonal in the new basis, since

$$\mathbf{b}^\dagger M \mathbf{b} = \Gamma^\dagger \mathbb{S}^\dagger M \mathbb{S} \Gamma = \Gamma^\dagger \mathbb{S}^\dagger \mathcal{I} \mathbb{S} \mathcal{I} D \Gamma = \Gamma^\dagger D \Gamma . \quad \text{(A12)}$$

Next, we note that the non-zero entries in A only connect two sites belonging to the same sublattice, while those in B always connect sites belonging to opposite sublattices. As a result of this, the solutions to the equation for y^μ can also be expressed in terms of a single function $f_\mu(\vec{r})$ defined on sites of the lattice. To see this, we consider an auxillary problem of finding $\tilde{\epsilon}_\mu$ such that the operator $A - B - \tilde{\epsilon}_\mu \eta_{\vec{r}}$ has a zero mode $f_\mu(\vec{r})$ (as before, $\eta_{\vec{r}}$ is +1 for sites belonging to the A sublattice, and -1 for sites belonging to the B sublattice).

This auxillary problem has N_{tot} solutions corresponding to the N_{tot} roots $\tilde{\epsilon}_\mu$ of the polynomial equation $\det(A - B - \tilde{\epsilon}_\mu \eta_{\vec{r}}) = 0$; these $\tilde{\epsilon}_\mu$ can be of either sign. To make the correspondence with the *positive* ϵ_μ solutions (u^μ, v^μ) (with $\mu = 1, 2 \ldots N_{\text{tot}}$) of the original equation $My^\mu = \epsilon_\mu \mathcal{I} y^\mu$, we now note that

$$\langle f_\mu | A - B | f_\mu \rangle = \tilde{\epsilon}_\mu N_\mu \quad \text{(A13)}$$

where

$$N_\mu \equiv \sum_{r_A} |f_\mu(r_A)|^2 - \sum_{r_B} |f_\mu(r_B)|^2. \quad \text{(A14)}$$

Since $A - B$ is a positive (but not positive definite) operator, this implies that $\tilde{\epsilon}_\mu$ has the same sign as N_μ for all non-zero $\tilde{\epsilon}_\mu$. To make the correspondence with the positive $\epsilon_\mu \equiv \lambda_\mu$ solutions ($\mu = 1, 2 \ldots N_{\text{tot}}$) of the original problem, we can therefore make the ansatz

$$u^\mu_{r_A} = f_\mu(r_A)/\sqrt{N_\mu}, u^\mu_{r_B} = 0 \quad \text{(A15)}$$
$$v^\mu_{r_B} = -f_\mu(r_B)/\sqrt{N_\mu}, v^\mu_{r_A} = 0$$

if $N_\mu > 0$, or the alternative ansatz

$$u^\mu_{r_B} = -f_\mu(r_B)/\sqrt{-N_\mu}, u^\mu_{r_A} = 0 \quad \text{(A16)}$$
$$v^\mu_{r_A} = f_\mu(r_A)/\sqrt{-N_\mu}, v^\mu_{r_B} = 0$$

if $N_\mu < 0$. Here, r_A (r_B) denotes sites belonging to the A (B) sublattice of the square lattice. This ansatz clearly ensures that the y^μ (with $\mu = 1, 2 .. N_{\text{tot}}$) obtained in this manner satisfy the original equation with positive $\epsilon_\mu \equiv \lambda_\mu$ and are appropriately normalized.

Atlhough this approach is not the one we use in our actual computations (see below), it provides a useful framework within which we may discuss possible zero frequency spin-wave modes, *i.e* $\lambda_{\mu_0} = 0$ for some μ_0: A mode μ_0 with $\lambda_{\mu_0} = 0$ clearly corresponds to a putative zero eigenvalue of the operator $A - B$. From the specific form of $A - B$ in our problem, it is clear that such a zero eigenvalue does indeed exist, and $f_{\mu_0}(\vec{r})$, the corresponding eigenvector of $A - B$, can be written down explicitly as

$$f_{\mu_0}(\vec{r}) = 1 \quad \text{(A17)}$$

Since this corresponds to the root $\tilde{\epsilon}_{\mu_0} = 0$ of the auxillary problem, it can *in principle* be used to obtain a *pair* of zero frequency modes ϵ_{μ_0} and $\epsilon_{\mu_0 + N_{\text{tot}}}$ for the original problem of finding ϵ_μ and y^μ that satisfy $My^\mu = \epsilon_\mu \mathcal{I} y^\mu$.

However, we need to ensure that the symplectic orthonormalization conditions (Eqn. A12) are satisfied by our construction of the corresponding y^{μ_0} and $y^{\mu_0 + N_{\text{tot}}}$. This is where the parity of $N_{\text{tot}} = L^2$ becomes important and we now restrict attention to odd N_{tot}. When N_{tot} is odd, *i.e.* when $N_A = N_B + 1$, we have $N_{\mu_0} = N_A - N_B = 1$. Thus, we are in a position to write down properly *normalized* zero-mode wavefunctions:

$$u^{\mu_0}_{r_A} = f_{\mu_0}(r_A), u^{\mu_0}_{r_B} = 0 \quad \text{(A18)}$$
$$v^{\mu_0}_{r_B} = -f_{\mu_0}(r_B), v^{\mu_0}_{r_A} = 0 ,$$

and

$$u^{N_{\text{tot}} + \mu_0}_r = v^{\mu_0}_r, \quad \text{(A19)}$$
$$v^{N_{\text{tot}} + \mu_0}_r = u^{\mu_0}_r .$$

[Parenthetically, we note that the question of zero frequency spin-wave modes for the more familiar case with $N_A = N_B$ and periodic boundary conditions has been discussed earlier in the literature.[14]]

Thus, the equation $My^\mu = \epsilon_\mu \mathcal{I} y^\mu$ has a pair of zero modes related to each other by interchange of the u and v components of the mode, and it becomes necessary to regulate intermediate steps of the calculation with a staggered magnetic field $\hat{z} \epsilon_h \eta_{\vec{r}}$ with infinitesimal magnitude $\epsilon_h > 0$ in the $\hat{z}$ direction. Denoting the corresponding A by A^{ϵ_h}, we see that $A^{\epsilon_h} - B$ is now a positive definite operator and does not have a zero eigenvalue. Indeed, it is easy to see from the foregoing that the corresponding eigenvalue now becomes non-zero, yielding a positive spin-wave frequency $\lambda^{\epsilon_h}_{\mu_0} = N_{\text{tot}} \epsilon_h$. One can also calculate the $\mathcal{O}(\epsilon_h)$ term of $f^{\epsilon_h}_{\mu_0}(\vec{r})$ and check that $f^{\epsilon_h}_{\mu_0}$ tends to $f_{\mu_0}(\vec{r})$ in a non-singular way as $\epsilon_h \to 0$, from which one can obtain the corresponding $y^{\mu_0}(\epsilon_h)$ analytically in this limit. Thus, the contribution of the zero mode to all physical quantities can be obtained in the presence of a small $\epsilon_h > 0$, and the $\epsilon_h \to 0$ limit of this contribution can then be taken smoothly and analytically at the end of the calculation.

In our actual calculations, we use this analytical understanding of the zero frequency spin-wave mode to analytically obtain the properly regularized zero mode contribution to various physical quantities, while using a computationally convenient approach to numerically calculate the contribution of the non-zero spin-wave modes. To do this, we rewrite Eqn. A5 for $\mu = 1, 2, 3 \ldots N_{\text{tot}}$ as

$$(A + B)\phi^\mu = \lambda_\mu \psi^\mu \quad \text{(A20)}$$
$$(A - B)\psi^\mu = \lambda_\mu \phi^\mu$$

where

$$\phi^\mu = u^\mu + v^\mu \quad \text{(A21)}$$
$$\psi^\mu = u^\mu - v^\mu .$$

This implies

$$(A - B)(A + B)\phi^\mu = \lambda_\mu(A - B)\psi^\mu = \lambda_\mu^2\phi^\mu \quad \text{(A22)}$$

$$(A + B)(A - B)\psi^\mu = \lambda_\mu(A + B)\phi^\mu = \lambda_\mu^2\psi_\mu \quad \text{(A23)}$$

We now decompose

$$A - B = K^\dagger K. \quad \text{(A24)}$$

where

$$K = \sqrt{\omega}U. \quad \text{(A25)}$$

with ω the diagonal matrix with diagonal entries given by eigenvalues of the real symmetric matrix $A-B$, and U the matrix whose rows are made up of the corresponding eigenvectors.

With this decomposition, we multiply Eqn A23 by K from the left to obtain

$$K(A + B)K^\dagger\chi^\mu = \lambda_\mu^2\chi^\mu. \quad \text{(A26)}$$

with $\chi^\mu = K\psi^\mu$. From the solution to this equation, we may obtain the ϕ as

$$\phi^\mu = (K^\dagger)\chi^\mu/\lambda_\mu. \quad \text{(A27)}$$

and thence obtain ψ^μ using Eqn A21. In order to ensure the correct normalization of the resulting u^μ, v^μ, we impose the normalization condition

$$(\chi^\mu)^\dagger\chi^\mu = \lambda_\mu. \quad \text{(A28)}$$

Thus our computational strategy consists of obtaining eigenvalues of the symmetric operator $K(A+B)K^\dagger$, and using this information to calculate the y^μ and thence the Bogoliubov transform matrix $\mathbb{S}$. Notwithstanding the normalization used in Eqn A28, the zero mode with $\lambda_{\mu_0} = 0$ causes no difficulties in this approach, since we work in practice with the projection of $K(A + B)K^\dagger$ in the space orthogonal to the zero mode. This is possible because we already have an analytic expression correct to $\mathcal{O}(\epsilon_h)$ for $y^{\mu_0}(\epsilon_h)$ and $y^{N_{\text{tot}}+\mu_0}(\epsilon_h)$ corresponding to this zero mode, and do *not* need to determine these two columns of $\mathbb{S}$ by this computational method.

We use this procedure to calculate the zero temperature boson density as

$$\langle b_{\vec{r}}^\dagger b_{\vec{r}} \rangle = \lim_{\epsilon_h \to 0} \sum_{\mu=1}^{N_{\text{tot}}} \left(v_{\vec{r}}^\mu(\epsilon_h)\right)^2. \quad \text{(A29)}$$

In this expression, one may use the numerical procedure outlined above to obtain the contribution of all $\mu \neq \mu_0$ *directly at* $\epsilon_h = 0$, while being careful to use our analytical results for $v^{\mu_0}(\epsilon_h)$ to obtain the limiting value of the contribution from $\mu = \mu_0$. This gives

$$\langle b_{\vec{r}_A}^\dagger b_{\vec{r}_A} \rangle = \sum_{\mu \neq \mu_0} (v_{\vec{r}_A}^\mu)^2 \quad \text{(A30)}$$

$$\langle b_{iB}^\dagger b_{iB} \rangle = 1 + \sum_{\mu \neq \mu_0} (v_{\vec{r}_B}^\mu)^2 \quad \text{(A31)}$$

Here, the distinction between sites on the A and B sublattices arises in this final result because $\lim_{\epsilon_h \to 0} v_{\vec{r}}^{\mu_0}(\epsilon_h) = -1$ for $\vec{r}$ belonging to the B sublattice, while $\lim_{\epsilon_h \to 0} v_{\vec{r}}^{\mu_0}(\epsilon_h) = 0$ for $\vec{r}$ belonging to the A sublattice. Knowing the average boson number at each site gives us the first quantum corrections to the ground state expectation value $\langle S^z(\vec{r}) \rangle$, as discussed in the main text.

Appendix B: Finite-size corrections to Δ

In order to reliably extrapolate to the thermodynamic limit and obtain Δ, we need to study the finite-size correction to Δ. In Fig. 9, we show a typical example of this size dependence. As is clear from this figure, we find that Δ has a non monotonic dependence on L: $\Delta(L)$ initially increases rapidly with size, and, after a certain crossover size L^*, it starts decreasing slowly to finally saturate to its asymptotic value, which we denote as Δ. This non-monotonic behaviour is qualitatively similar to that observed in the finite size extrapolations of n^z from our QMC data earlier. To explore this unusual size dependence further and reliably extrapolate to the thermodynamic limit, we analyze the contributions to the finite-size $\Delta(L)$ from the spin-wave spectrum in the following way: We note that there is always a monotonically and rapidly convergent $\mathcal{O}(1)$ contribution to $\Delta(L)$ from the lowest frequency spin-wave mode, whose spin-wave frequency scales to zero as $1/N_{\text{tot}}$ (for any finite N_{tot}, this is *not* an exact zero mode of the system). We dub this the 'delta-function contribution', and note that it is easy to reliably extrapolate this contribution to the thermodynamic limit. In addition, there is a 'continuum contribution' coming from all the other spin-wave modes, each of which contributes an amount of order $\mathcal{O}(1/N_{\text{tot}})$. This contribution converges less rapidly to the thermodynamic limit, and also happens to be non-monotonic: it first increases quickly with increasing size, and then starts decreasing slowly to finally saturate to the thermodynamic limit.

The delta-function contribution can be fit best to a functional form

$$F_\delta(L) = b_\delta + \frac{c_\delta}{L} - \frac{a_\delta}{L^2} + \frac{d_\delta}{L^3}, \quad \text{(B1)}$$

with the dominant $1/L^2$ term accounting for the monotonic increase with L, while the continuum contribution is fit to

$$F_c(L) = b_c + \frac{c_c}{L} - \frac{a_c}{L^2} + \frac{d_c}{L^3}, \quad \text{(B2)}$$

whereby the size dependence is predominantly determined by the competition between the term proportional to $1/L$ which decreases with increasing L, and the term
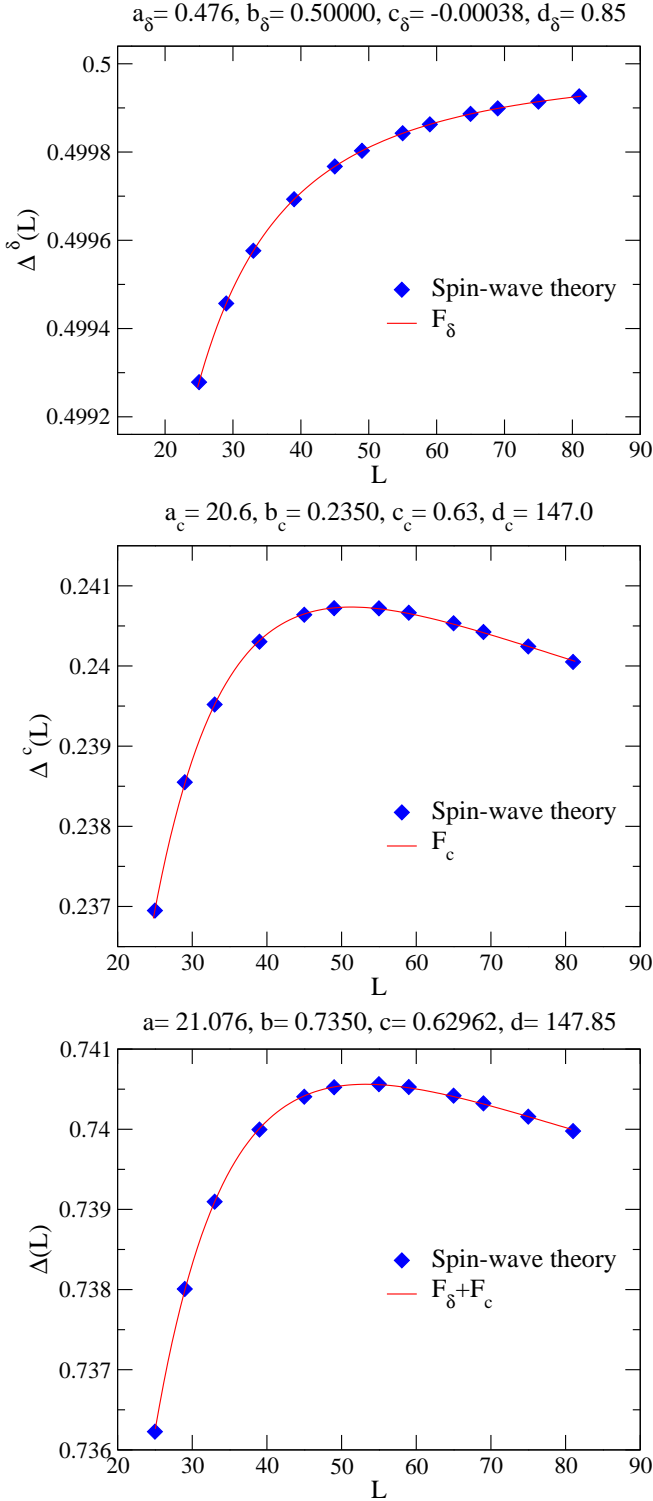
FIG. 9. A typical example of the finite-size corrections to the delta-function and continuum contributions to Δ. Note the monotonically increasing size dependence of the delta-function contribution, and the non-monotonic and more slowly converging nature of the continuum contribution. Due to this difference in their behaviour, we find it more accurate to separately fit each of these contributions to a polynomial in $1/L$ and use this to obtain Δ in the thermodynamic limit. Here $F_{\delta/c}(L) = b_{\delta/c} + c_{\delta/c}/L - a_{\delta/c}/L^2 + d_{\delta/c}/L^3$. In the last figure a, b, c and d are obtained by $a = a_\delta + a_c$, $b = b_\delta + b_c$, $c = c_\delta + c_c$ and $d = d_\delta + d_c$.

proportional to $1/L^2$ which increases with increasing L. This gives rise to non-monotonic behaviour whereby the continuum contribution first increases rapidly and then decreases slowly beyond a crossover length L^* to finally saturate to its infinite volume limit. We also find that the length L^* gets larger as we deform away from the pure square lattice antiferromagnet, making it harder to obtain reliable extrapolations to the thermodynamic limit. Nevertheless, for all data shown in the main text, we have gone to large enough L to be fairly confident of the extrapolation to the thermodynamic limit, and the systematic errors associated with this extrapolation are estimated to be small enough to not affect our conclusions.

[1] H. Neuberger and T. Ziman, Phys. Rev. B **39**, 2608(1989).

[2] A. W. Sandvik, Phys. Rev. B **56**, 11678 (1997).

[3] B. B. Beard, R. J. Birgeneau, M. Greven, and U.-J. Wiese, Phys. Rev. Lett. **80**, 1742 (1998).

[4] S. R. White and A. L. Chernyshev, Phys. Rev. Lett. **99**, 127004 (2007).

[5] E. Lieb and D. C. Mattis, J. Math. Phys. **3**, 749 (1962).

[6] K. Hoglund Ph.D thesis (2010); K. Hoglund and A. W. Sandvik, unpublished.

[7] S. Wenzel and W. Janke, Phys. Rev. B**79**, 014410(2009).

[8] A. W. Sandvik, Phys. Rev. Lett. **98**, 227202 (2007).

[9] J. Lou, A. W. Sandvik, and N. Kawashima, Phys. Rev. B **80**, 180414 (2009).

[10] A. Banerjee and K. Damle, J. Stat. Mech. (2010) P08017.

[11] A. W. Sandvik, Phys. Rev. Lett. **95**, 207203 (2005).

[12] A. W. Sandvik, and H. G. Evertz, Phys. Rev. B **82**, 024407 (2010).

[13] A. W. Sandvik, Phys. Rev. Lett. **83**, 3069 (1999).

[14] P. W. Anderson, Phys. Rev. **86**, 694 (1952).

[15] P. Chandra and B. Doucot, Phys. Rev. B **38**, 9335, 1988

[16] J. H. P. Colpa, Physica A **2**, 134, 377-416 (1986); J. H. P. Colpa, Physica A **2**, 134, 417-422 (1986)

[17] S. Chandrasekharan, F.-J. Jiang, M. Pepe, and U.-J. Wiese, Phys. Rev. D **78**, 077901 (2008).

[18] T. T. Wu and C. N. Yang, Nuc. Phys. **B107**, 365 (1976); Phys. Rev. D **16**, 1018 (1977).

[19] S. Eggert, O.F. Syliuåsen, F. Anfuso, M.Andres, Phys. Rev. Lett. **99**, 097204 (2007).